

A Synthetic Model for the Putative Fe^{IV}₂O₂ Diamond Core of Methane Monooxygenase Intermediate Q

Miquel Costas,[†] Jan-Uwe Rohde,[†] Audria Stubna,[‡]
Raymond Y. N. Ho,[†] Luca Quaroni,[†] Eckard Münck,^{*,‡} and
Lawrence Que, Jr.^{*,†}

Department of Chemistry and Center for Metals in
Biocatalysis, University of Minnesota, 207 Pleasant Street SE
Minneapolis, Minnesota 55455

Department of Chemistry, Carnegie Mellon University
Pittsburgh, Pennsylvania 15213

Received October 1, 2001

High valent iron-oxo intermediates are frequently invoked as the key oxidants in the oxygen activation mechanisms of iron enzymes that carry out the two-electron oxidations of alkanes to alcohols and of olefins to epoxides.^{1,2} Such high-valent intermediates have been characterized in heme enzymes and are best described as an oxoiron(IV) porphyrin ligand radical complex.^{1,3} The corresponding intermediate for the soluble diiron enzyme methane monooxygenase (MMO) is a diiron(IV) species called Q.⁴ EXAFS analysis reveals a short Fe–Fe distance of 2.5 Å, which has led us to propose an Fe₂O₂ diamond core structure.⁵ Model compounds have played an important role in establishing the credibility of the [Fe^{IV}(O)(porphyrin radical)]⁺ description for the heme enzyme intermediate;⁶ however, our current understanding of MMO-Q is at a more rudimentary stage, due in part to the paucity of appropriate model compounds. While DFT calculations from a number of groups support the stability of such an Fe^{IV}₂(μ-O)₂ core,⁷ to date there is only one structurally characterized high-valent model complex with an Fe₂O₂ diamond core,⁸ namely [Fe₂(μ-O)₂(5-Et₃-TPA)₂](ClO₄)₃.⁹ However, this complex has an Fe^{III}Fe^{IV} oxidation state, which is one-electron reduced relative to that of MMO-Q. Our synthetic efforts have led us to explore ligands related to the TPA framework, and in this report we provide evidence for the generation of a diiron(IV) complex with an Fe₂O₂ diamond core.

A precursor to the diiron(IV) complex is the mononuclear iron(II) complex [Fe(BPMCN)(OTf)₂] (**1**). The crystal structure of the 5-methyl-substituted analogue shows a six-coordinate iron(II) site with the two triflates bound cis to each other and the tetradentate BPMCN ligand wrapped around the iron such that the two pyridines are also coordinated cis to each other (Figure 1, see Supporting Information for further details). Complex **1** is

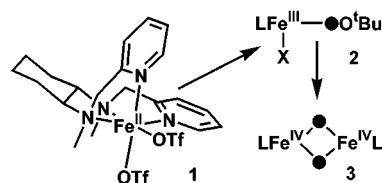


Figure 1. Formation of diiron(IV) complex **3** from **1**.

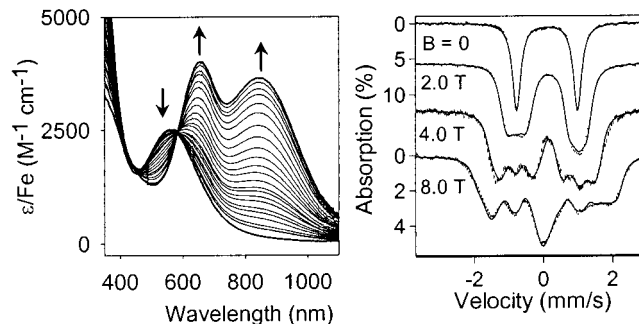


Figure 2. Left panel: Conversion of **2** to **3** in CH₂Cl₂ at –80 °C as monitored by UV–vis spectroscopy over a 16 h period with $t_{1/2} \sim 4$ h. Right panel: Mössbauer spectra of ⁵⁷Fe-enriched **3** recorded at 4.2 K in zero field (top) and in parallel applied fields as indicated. The solid lines are simultaneous fits to groups of four spectra based on the spin Hamiltonian for a symmetric exchange coupled Fe^{IV}Fe^{IV} dimer with $S_1 = S_2 = 1$ for $J = -5$ cm⁻¹. $H = JS_1 \cdot S_2 + \sum_{i=1}^2 \{S_i \cdot D_i \cdot S_i + \beta S_i \cdot g_i \cdot B + S_i \cdot A_i \cdot I_i - g_i \beta_n B \cdot I_i + H_Q(i)\}$. For each site the A-tensor ($A_x = -30.2$ MHz, $A_y = -23.6$ MHz, $A_z = -1.5$ MHz) is tilted by Euler angles α , β , γ (73°, 111°, 163°) with respect to the ZFS tensor ($D = +19$ cm⁻¹, $E/D = 0.15$), while the EFG tensor ($\Delta E_Q = +1.75$ mm/s, $\eta = 0.8$) is rotated by (85°, 107°, 210°) relative to the ZFS-tensor.

isostructural, based on the similarity of their ¹H NMR spectra (Figure S1).

Treatment of **1** in CH₂Cl₂ solution at –80 °C with 10 equiv of ^tBuOOH (5–6 M in nonane) results in the immediate formation of a blue species **2** (λ_{max} 566 nm, $\epsilon \sim 2500$ M⁻¹ cm⁻¹) with EPR, Mössbauer, and Raman properties that identify it as an Fe^{III}-OO^tBu complex, like those previously described for related Fe(TPA) complexes.¹⁰ Upon standing at –80 °C, **2** converts monotonically to metastable **3** with intense absorption features at 656 and 845 nm (Figure 2, left). Addition of pentane allows **3** to be precipitated at –80 °C; this solid affords an elemental analysis that establishes **3** to have an Fe:ligand:OTf ratio of 1:1:2 (% C 37.17, % H 4.70, % Fe 7.18, % F 14.57, % N 7.10, % S 8.02; see Supporting Information).

The 4.2 K Mössbauer spectrum of **3** in butyronitrile exhibits a single sharp quadrupole doublet with $\delta = 0.10$ mm/s and $\Delta E_Q = 1.75$ mm/s (Figure 2, right). Spectra recorded between 4.2 and 100 K in applied fields of up to 8.0 T are characteristic of an integer spin paramagnet with a large positive zero-field splitting (ZFS). The hyperfine parameters of **3** compare favorably with those of $S = 1$ Fe^{IV} sites found in porphyrin¹¹ and non-porphyrin complexes.¹² Our data set (11 spectra) can be fit very well either to (i) a mononuclear $S = 1$ Fe^{IV} species or (ii) a symmetric exchange-coupled Fe^{IV}Fe^{IV} dimer ($H = JS_1 \cdot S_2$, $S_1 = S_2 = 1$) provided that $|J| < 5$ cm⁻¹. Figure 2 (right) shows theoretical

(10) Zang, Y.; Kim, J.; Dong, Y.; Wilkinson, E. C.; Appelman, E. H.; Que, L., Jr. *J. Am. Chem. Soc.* **1997**, *119*, 4197–4205.

(11) Gold, A.; Jayaraj, K.; Doppelt, P.; Weiss, R.; Chottard, G.; Bill, E.; Ding, X.; Trautwein, A. X. *J. Am. Chem. Soc.* **1988**, *110*, 5756–5761.

(12) (a) Grapperhaus, C. A.; Mienert, B.; Bill, E.; Weyhermüller, T.; Wieghardt, K. *Inorg. Chem.* **2000**, *39*, 5306–5317. (b) Meyer, K.; Bill, E.; Mienert, B.; Weyhermüller, T.; Wieghardt, K. *J. Am. Chem. Soc.* **1999**, *121*, 4859–4876.

[†] University of Minnesota.

[‡] Carnegie Mellon University.

(1) Sono, M.; Roach, M. P.; Coulter, E. D.; Dawson, J. H. *Chem. Rev.* **1996**, *96*, 2841–2887.

(2) Wallar, B. J.; Lipscomb, J. D. *Chem. Rev.* **1996**, *96*, 2625–2658.

(3) Schlichting, I.; Berendzen, J.; Chu, K.; Stock, A. M.; Maves, S. A.; Benson, D. E.; Sweet, R. M.; Ringe, D.; Petsko, G. A.; Sligar, S. G. *Science* **2000**, *287*, 1615–1622.

(4) (a) Lee, S.-K.; Nesheim, J. C.; Lipscomb, J. D. *J. Biol. Chem.* **1993**, *268*, 21569–21577. (b) Lee, S.-K.; Fox, B. G.; Froland, W. A.; Lipscomb, J. D.; Münck, E. *J. Am. Chem. Soc.* **1993**, *115*, 6450–6451. (c) Liu, K. E.; Valentine, A. M.; Wang, D.; Huynh, B. H.; Edmondson, D. E.; Salifoglou, A.; Lippard, S. J. *J. Am. Chem. Soc.* **1995**, *117*, 10174–10185.

(5) Shu, L.; Nesheim, J.; Kauffmann, K.; Münck, E.; Lipscomb, J. D.; Que, L., Jr. *Science* **1997**, *275*, 515–518.

(6) Groves, J. T.; Han, Y.-Z. In *Cytochrome P450: Structure, Mechanism, and Biochemistry*, 2nd ed.; Ortiz de Montellano, P. R., Ed.; Plenum Press: New York, 1995; pp 3–48.

(7) (a) Dunietz, B. D.; Beachy, M. D.; Cao, Y.; Whittington, D. A.; Lippard, S. J.; Friesner, R. A. *J. Am. Chem. Soc.* **2000**, *122*, 2828–2839. (b) Siegbahn, P. E. M. *Inorg. Chem.* **1999**, *38*, 2880–2889. (c) Siegbahn, P. E. M.; Crabtree, R. H. *J. Am. Chem. Soc.* **1997**, *119*, 3103–3113. (d) Basch, H.; Mogi, K.; Musaev, D. G.; Morokuma, K. *J. Am. Chem. Soc.* **1999**, *121*, 7249–7256.

(8) Hsu, H.-F.; Dong, Y.; Shu, L.; Young, V. G., Jr.; Que, L., Jr. *J. Am. Chem. Soc.* **1999**, *121*, 5230–5237.

(9) Abbreviations used: 5-Et₃-TPA = tris(5-ethyl-2-pyridylmethyl)amine; BPMCN = *N,N'*-bis(2-pyridylmethyl)-*N,N'*-dimethyl-*trans*-1,2-diaminocyclohexane; OTf = CF₃SO₃⁻.

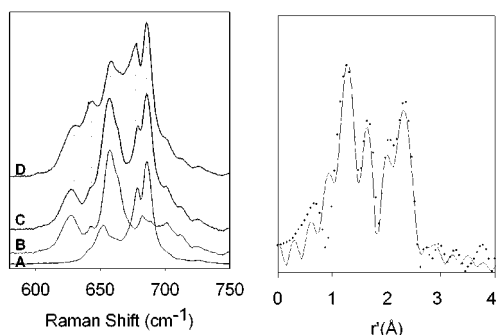


Figure 3. Left panel: Resonance Raman spectra of **3** obtained in frozen methanol solution with 632.8 nm excitation: A, from ${}^1\text{Bu}^{16}\text{O}^{16}\text{OH}$; B, from ${}^1\text{Bu}^{16}\text{O}^{18}\text{OH}$; C, computer generated sum of A and B; D, from a mixture of ${}^1\text{Bu}^{16}\text{O}^{16}\text{OH}$ and ${}^1\text{Bu}^{16}\text{O}^{18}\text{OH}$. Right panel: Fourier transform of the Fe K-edge EXAFS data (\cdots) and fit ($-$) in r' space of **3** (k , 2–13.5 \AA^{-1}) in frozen butyronitrile solution. Fitting: 1 O at 1.79 \AA ($\Delta\sigma^2$, -0.0007\AA^2), 3 N at 1.99 \AA ($\Delta\sigma^2$, 0.0038\AA^2), 1 Fe at 2.81 \AA ($\Delta\sigma^2$, 0.009\AA^2), and 7 C at 2.92 \AA ($\Delta\sigma^2$, 0.010\AA^2).

spectra based on case (ii); details are given in the Supporting Information.

We have also fit the Mössbauer spectra to models involving high-spin ($S = 2$) Fe^{IV} sites; these attempts, however, yielded unreasonably small values for the isotropic part of the A-tensor, e.g. $A_{\text{iso}} = -6$ MHz compared to $A_{\text{iso}} \sim -22$ MHz observed for the high-spin Fe^{IV} sites of $[\text{Fe}^{\text{III}}\text{Fe}^{\text{IV}}(\text{O})_2(\text{L})_2](\text{ClO}_4)_3$ ($\text{L} = 6\text{-Me-TPA}$ or $6\text{-Me}_3\text{-TPA}$).^{13,14} Fits to an exchange-coupled dimer comprising low-spin ($S_1 = S_2 = 1/2$) Fe^{III} sites required an unreasonably large $A_{\text{iso}} = -36$ MHz. (For comparison, low-spin Fe^{III} complex **2** has $A_{\text{iso}} = -17.7$ MHz, a value typical for this type of coordination environment). Thus, if **3** is formulated as a dimer, it must be $\text{Fe}^{\text{IV}}\text{Fe}^{\text{IV}}$.

The resonance Raman spectrum of **3** in MeOH shows features at 686, 679, and 653 cm^{-1} (Figure 3A), which downshift to 658 and 627 cm^{-1} when ${}^1\text{Bu}^{16}\text{O}^{18}\text{OH}$ is used (Figure 3B). The vibrations must thus arise from a species that incorporates the terminal oxygen atom of ${}^1\text{BuOOH}$. The observed downshifts of 23–26 cm^{-1} approach the 30 cm^{-1} value calculated from Hooke's law for an Fe–O vibration. Given the Mössbauer evidence for an Fe^{IV} site, a terminal $\text{Fe}^{\text{IV}}=\text{O}$ assignment for **3** immediately comes to mind, but the Fe–O vibrations for such species are usually observed between 800 and 850 cm^{-1} .^{14,15} Interestingly, oxygen-isotope sensitive vibrations in the 600–700 cm^{-1} region are the spectroscopic signature for an $\text{M}_2(\mu\text{-O})_2$ diamond core.¹⁶ If **3** has a diamond core, the complex must contain the terminal oxygen atoms derived from two ROOH units. This is indeed the case as experiments on **3**, generated with a mixture of ${}^1\text{Bu}^{16}\text{O}$ -

(13) Dong, Y.; Que, L., Jr.; Kauffmann, K.; Münck, E. *J. Am. Chem. Soc.* **1995**, *117*, 11377–11378.

(14) Zheng, H.; Yoo, S. J.; Münck, E.; Que, L., Jr. *J. Am. Chem. Soc.* **2000**, *122*, 3789–3790.

(15) Kitagawa, T.; Mizutani, Y. *Coord. Chem. Rev.* **1994**, *135/136*, 685–735.

(16) (a) Wilkinson, E. C.; Dong, Y.; Zang, Y.; Fujii, H.; Fraczkiewicz, R.; Fraczkiewicz, G.; Czernuszewicz, R. S.; Que, L. Jr. *J. Am. Chem. Soc.* **1998**, *120*, 955–962. (b) Henson, M. J.; Mukherjee, P.; Root, D. E.; Stack, T. D. P.; Solomon, E. I. *J. Am. Chem. Soc.* **1999**, *121*, 10332–10345. (c) Holland, P.; Cramer, C. J.; Wilkinson, E. C.; Mahapatra, S.; Rodgers, K. R.; Itoh, S.; Taki, M.; Fukuzumi, S.; Que, L., Jr.; Tolman, W. B. *J. Am. Chem. Soc.* **2000**, *122*, 792–802.

${}^{16}\text{OH}$ and ${}^1\text{Bu}^{16}\text{O}^{18}\text{OH}$ (Figure 3D), reveal additional vibrations at intermediate frequencies that are absent in the combined spectra of the pure ${}^{16}\text{O}$ and ${}^{18}\text{O}$ isotopomers (Figure 3C).

The Fe K-edge EXAFS spectrum of **3** also supports the presence of an $\text{Fe}_2(\mu\text{-O})_2$ diamond core (Figure 3 right, see Supporting Information for k -space data and fit). The best fit to the data consists of four shells: 1 O at 1.79 \AA , 3 N at 1.99 \AA , 1 Fe at 2.81 \AA , and 7 C at 2.92 \AA , parameters comparable to those found for the crystallographically characterized $[\text{Fe}_2(\mu\text{-O})_2(5\text{-Et}_3\text{-TPA})_2](\text{ClO}_4)_3$.⁸ Thus the 1.79 \AA shell is associated with the oxo bridges of the diamond core, the 1.99 \AA shell with the N atoms of the BPMCN ligand bound to low-spin Fe^{IV} , and the 2.92 \AA shell with the carbon atoms adjacent to the ligating nitrogen atoms. The 2.81 \AA Fe–Fe distance attributed to **3** is well within the 2.6–2.9 \AA range of metal–metal distances found for high-valent $\text{M}_2(\mu\text{-O})_2$ complexes.¹⁷ Taken together, **3** can thus be formulated as $[\text{Fe}_2\text{O}_2(\text{BPMCN})_2](\text{OTf})_4$.

The reactivity of isolated **3** toward hydrocarbon substrates significantly differs from that of $[\text{Fe}_2(\mu\text{-O})_2(\text{TPA})_2](\text{ClO}_4)_3$. The latter $\text{Fe}^{\text{III}}\text{Fe}^{\text{IV}}$ complex acts as a one-electron oxidant, and reacts only with substrates containing activated C–H bonds such as ethylbenzene and cumene.¹⁸ In contrast, **3** acts as a two-electron oxidant and oxidizes hydrocarbons with stronger C–H bonds. For example, at -40 $^\circ\text{C}$ and under Ar, **3** reacts with adamantane to afford 1-adamantanol and 2-adamantanone in 56% and 20% yield, respectively. Thus **3** can attack unactivated aliphatic C–H bonds, commensurate with the expected higher oxidizing power of its diiron(IV) oxidation state.

To date, **3** represents the closest analogue of MMO-Q, mimicking key aspects of its core structure and hydrocarbon oxidizing ability. However, there are key differences in the iron spin state and ligand environment (the Fe^{IV} sites of MMO-Q are high spin⁴ and carboxylate-rich¹⁹) that yield J -values and optical bands that differ from those observed for MMO-Q. Nevertheless, the synthesis and isolation of **3** attest to the chemical viability of an $\text{Fe}^{\text{IV}}_2\text{O}_2$ diamond core structure, lending credence to the assignment of such a core structure for MMO-Q.

Acknowledgment. This work was supported by NIH Grants GM-38767 to L.Q. and GM-22701 to E.M. M.C. and J.-U.R. thank Fundacio La Caixa and the Deutsche Forschungsgemeinschaft (DFG), respectively, for postdoctoral fellowships. XAS data were collected on beamline X9B at the National Synchrotron Light Source and at beamline 7-3 of the Stanford Synchrotron Radiation Laboratory, both supported by the US Department of Energy and the NIH Research Resource program. We thank Dr. Victor Young and Dr. Maren Pink of the University of Minnesota X-ray Crystallographic Laboratory for the crystal structure of $[\text{Fe}(5\text{-Me}_2\text{-BPMCN})(\text{OTf})_2]$.

Supporting Information Available: X-ray crystallographic file for $[\text{Fe}(5\text{-Me}_2\text{-BPMCN})(\text{OTf})_2]$ (CIF); experimental procedures for **1** and **3**, ${}^1\text{H}$ NMR spectra of **1** and $[\text{Fe}(5\text{-Me}_2\text{-BPMCN})(\text{OTf})_2]$, and details for the Mössbauer and EXAFS analysis of **3** (PDF). This material is available free of charge via the Internet at <http://pubs.acs.org>.

JA017204F

(17) Que, L., Jr.; Tolman, W. B. *Angew. Chem., Int. Ed.* Accepted for publication.

(18) Kim, C.; Dong, Y.; Que, L., Jr. *J. Am. Chem. Soc.* **1997**, *119*, 3635–3636.

(19) Merckx, M.; Kopp, D. A.; Sazinsky, M. H.; Blazyk, J. L.; Müller, J.; Lippard, S. J. *Angew. Chem., Int. Ed.* **2001**, *40*, 2782–2807.